was compensated electronically, thus reducing the maximum error of the voltage clamp to approximately 10 mV for the largest currents recorded (~10 nA). The intracellular solution contained 120 mM K-glutamate, 20 mM KCl, 10 mM Hepes, 0.02 to 0.03 mM Calcium Green (Molecular Probes, Eugene, OR), 10 mM Na^+, 5.5 mM total Mg, and 0.2, 1, or 5 mM ATP (Na^+ and Mg^{2+} concentrations were held constant with Na^+ or Mg^{2+} salts of ATP; pipette pH adjusted to 7.2 with KOH). Calcium Green was replaced with EGTA when NADH fluorescence was measured. In some experiments, 1 mM caged ATP or 1 mM caged ADP were added to the pipette solution and photolyzed with a xenon flash lamp. A continuous xenon arc lamp was used to provide excitation light (485 nm) for Calcium Green; fluorescence emission (530 nm) was detected with a photomultiplier tube. NADH fluorescence was measured at 460 nm in myocytes illuminated with 350 nm ultraviolet light. Membrane ionic currents and fluorescence signals were acquired by a digital interface controlled by a personal computer and customized software. Experiments were done in accordance with institutional guidelines regarding the care and use of animals.

9. B. Belles, C. O. Malécot, J. Hescheler, W. Trautwein, *Pflueg. Arch.* **411**, 353 (1988).
10. In the majority of the experiments, the frequency and amplitude of the spontaneous oscillations remained constant over long periods of time and could be approximated by a sinusoidal function; however, in several instances, an additional frequency damping factor of 10 to 20% over a 10-min time period was needed to adequately describe the data. A few cells displayed oscillations with an irregular phase, amplitude, or both (Fig. 3A). These examples of unusual patterns of oscillation are similar to those observed in cell-free extracts when the substrate influx rate is altered and may be explained by variability in the amounts of endogenous energy stores in the isolated myocytes. Glycogen, which is partially depleted by the isolation process [V. Chen, K. H. McDonough, J. J. Spitzer, *Biochim. Biophys. Acta* **846**, 398 (1985)], presumably supports the cyclical alterations in metabolic rate by providing substrate at a slower rate than in the presence of glucose. Differences in rates of glucose transport or glycogenolysis among cells may account for the variable sensitivities to external glucose. The reduction in amplitude of the Ca^{2+} transients could result from nucleotide-dependent regulation of L-type Ca^{2+} channels [B. O'Rourke, P. H. Backx, E. Marban, *Science* **257**, 245 (1992)], sarcoplasmic reticulum Ca^{2+} release channels [G. Meissner and J. S. Henderson, *J. Biol. Chem.* **262**, 3065 (1987)], or metabolite effects on ATP-dependent ion pumps.
11. The oscillations in Ca^{2+} transient amplitude were also eliminated after $I_{K,ATP}$ blockade (Fig. 2B). This may indicate that the primary intracellular oscillator is influenced by surface membrane events, perhaps as a result of secondary ATP consumption by ion pumps such as the Na^+, K^+ ATPase. Tight coupling between Na^+, K^+ ATPase–mediated changes in intracellular ATP and K,ATP channel activity has been demonstrated in the renal proximal tubule [K. Tsuchiya, W. Wang, G. Giebisch, P. A. Welling, *Proc. Natl. Acad. Sci. U.S.A.* **89**, 6418 (1992)]. A second possibility is that glibenclamide may have metabolic effects in addition to its ability to inhibit K,ATP channels [M. Gwilt, B. Norton, C. G. Henderson, *Eur. J. Pharmacol.* **236**, 107 (1993)]. Although there are many alternative explanations as to why inhibiting K^+ efflux halted the oscillations in Ca^{2+} transient amplitude, it is important to note that the reverse was not true, that is, eliminating the Ca^{2+} transients did not eliminate the membrane current oscillations (see Fig. 2C).
12. A. A. Kort, E. G. Lakatta, E. Marban, M. D. Stern, W. G. Wier, *J. Physiol. (London)* **367**, 291 (1985).
13. P. E. Rapp and M. J. Berridge, *J. Theor. Biol.* **66**, 497 (1977).
14. K.-G. Collatz and M. Horning, *Comp. Biochem. Physiol.* **96**, 771 (1990).
15. R. Frenkel, *Arch. Biochem. Biophys.* **125**, 157 (1968).
16. J. Eng, R. M. Lynch, R. S. Balaban, *Biochem. J.* **55**, 621 (1989).
17. V. D. Gooch and L. Packer, *Biochim. Biophys. Acta* **346**, 245 (1974).
18. L. Stryer, *Biochemistry* (Freeman, San Francisco, CA, 1981).
19. The relative ineffectiveness of the ATP in the pipette solution (for example, 5 mM MgATP used in Fig. 1, A and B) to prevent the oscillations and the absence of a rise in the holding current when glycolysis was inhibited with 2-deoxyglucose (Fig. 4D) suggest that the cyclical activation of $I_{K,ATP}$ did not result from subsarcolemmal deprivation of glycolytically derived ATP, but rather from the oscillatory generation of $I_{K,ATP}$ activators such as ADP [J. N. Weiss, N. Venkatesh, S. T. Lamp, *J. Physiol. (London)* **447**, 649 (1992)], AMP, lactate [E. C. Keung, Q. Li, *J. Clin. Invest.* **88**, 1772 (1991)], or protons [W. J. Lederer and C. G. Nichols, *J. Physiol. (London)* **419**, 193 (1989)]. Changes in the concentration of ATP during oscillations in glycolysis (two- to threefold) are much less than those in other intermediates like AMP (20-fold) or fructose 1,6-diphosphate (40-fold) (*4*).
20. A. L. Wit and M. J. Janse, *The Ventricular Arrhythmias of Ischemia and Infarction: Electrophysiological Mechanisms* (Futura, Mount Kisco, NY, 1993).
21. B. Hess, *Hoppe-Seyler's Z. Physiol. Chem.* **364**, 1 (1983).
22. A. Boiteux, A. Goldbeter, B. Hess, *Proc. Natl. Acad. Sci. U.S.A.* **72**, 3829 (1975).
23. M. Markus, D. Kuschmitz, B. Hess, *FEBS Lett.* **172**, 235 (1984).
24. M. A. Aon *et al.*, *J. Cell Sci.* **99**, 325 (1991).
25. K. Tornheim and J. M. Lowenstein, *J. Biol. Chem.* **249**, 3241 (1974).
26. A. Ghosh and B. Chance, *Biochem. Biophys. Res. Commun.* **16**, 174 (1964).
27. B. Chance, B. Schoener, S. Elsaesser, *J. Biol. Chem.* **240**, 3170 (1965); R. Frenkel, *Arch. Biochem. Biophys.* **115**, 112 (1966); B. Chance, B. Schoener, S. Elsaesser, *Biochemistry* **52**, 337 (1964).
28. Results similar to those shown in Fig. 5B were observed in response to photolytic release of ADP in four other cells. When ADP was released during maintained oscillations, phase alterations that included double periodicities were observed. ATP release from caged ATP also induced oscillations in eight cells, but the oscillations began after a longer delay from the time of the flash. Both ADP and ATP influence oscillations in cell-free extracts of glycolytic enzymes (*27*). The delayed effect of ATP may result from its hydrolysis to ADP. Approximately 10% of caged ADP is released by photolysis under optimal conditions and would be likely to be removed within seconds [Y. E. Goldman, M. G. Hibberd, J. A. McCray, D. R. Trentham, *Nature* **300**, 701 (1982)]. The prolonged oscillatory response to the transient perturbation of intracellular nucleotides by flash photolysis is predicted by models of the glycolytic oscillator [A. Goldbeter, in *Mathematical Models in Molecular and Cellular Biology* (Cambridge Univ. Press, Cambridge, 1980), pp. 260–291].

29. We thank A. P. Thomas and W. G. Wier for comments on the manuscript. Supported by NIH grant #RO1 HL 36957.

26 January 1994; accepted 8 July 1994

Transformation of Mammalian Cells by Constitutively Active MAP Kinase Kinase

Sam J. Mansour, Wayne T. Matten, April S. Hermann, Julian M. Candia, Sing Rong, Kenji Fukasawa, George F. Vande Woude, Natalie G. Ahn*

Mitogen-activated protein (MAP) kinase kinase (MAPKK) activates MAP kinase in a signal transduction pathway that mediates cellular responses to growth and differentiation factors. Oncogenes such as *ras, src, raf*, and *mos* have been proposed to transform cells by prolonging the activated state of MAPKK and of components downstream in the signaling pathway. To test this hypothesis, constitutively active MAPKK mutants were designed that had basal activities up to 400 times greater than that of the unphosphorylated wild-type kinase. Expression of these mutants in mammalian cells activated AP-1–regulated transcription. The cells formed transformed foci, grew efficiently in soft agar, and were highly tumorigenic in nude mice. These findings indicate that constitutive activation of MAPKK is sufficient to promote cell transformation.

Cell transformation often results from constitutive activation of components in signaling pathways that control cell proliferation and differentiation. These pathways are initiated from various cell surface receptors, and many converge on the MAP kinase cascade, a module consisting of MAPKK (also known as MAPK or ERK kinase, or as MEK), mitogen-activated protein kinase (MAPK, also known as extracellular signal-regulated kinase or ERK), and pp90 ribosomal protein S6 kinase ($pp90^{rsk}$). These kinases form three successive tiers of a cascade in which MAPKK phosphorylates and activates MAPK, and MAPK phosphorylates and activates $pp90^{rsk}$ (*1*, *2*).

Cellular forms of several viral oncogenes are found as signaling components upstream and downstream of the MAP kinase cascade, which suggests that the pathway mediates cell transformation. Proto-oncogene products upstream of the cascade include

S. J. Mansour, Department of Chemistry and Biochemistry and Department of Molecular, Cellular, and Developmental Biology, University of Colorado, Boulder, CO 80309, USA.
A. S. Hermann, J. M. Candia, N. G. Ahn, Howard Hughes Medical Institute, Department of Chemistry and Biochemistry, University of Colorado, Boulder, CO 80309, USA.
W. T. Matten, S. Rong, K. Fukasawa, G. F. Vande Woude, Advanced BioSciences Laboratories–Basic Research Program, National Cancer Institute–Frederick Cancer Research and Development Center, Frederick, MD 21702, USA.
*To whom correspondence should be addressed.

receptor tyrosine kinases, c-Src, Ras, and the $G_{\alpha i}$ subunit of heterotrimeric G proteins (*3*). In addition, the proto-oncogene protein kinases Raf-1 and c-Mos phosphorylate and activate MAPKK (*4*, *5*). Proto-oncogene products downstream of the MAP kinase cascade include the transcription factors c-Jun, c-Fos, c-Myc, and c-Myb, which are substrates for phosphorylation by MAPK or $pp90^{rsk}$ (*6*). After cell stimulation, both MAPK and $pp90^{rsk}$ translocate to the nucleus (*7*) where they are believed to regulate gene transcription (*6*, *8*, *9*).

Activation of the MAP kinase cascade appears to be necessary for cell growth. Growth factor–regulated gene transcription and cell proliferation are blocked in mammalian cells by expression or microinjection of dominantly interfering mutants of MAPK or of antisense RNA complementary to MAPK transcripts (*10*, *11*). These studies indicate that MAPKK and MAPK are necessary components, but the sufficiency of the MAP kinase cascade as a regulator of cell growth remains unproven. In particular, oncogenic forms of MAPKK and MAPK have never been found, which suggests that deregulation of alternate signaling pathways may be required for cell transformation.

We designed constitutively active mutants of MAPKK with basal activities up to several hundred times greater than that of the wild-type enzyme. Activation of MAPKK by Raf-1 or v-Mos occurred through the phosphorylation of two key regulatory sites, Ser^{218} and Ser^{222} (Fig. 1A) (*12*). After substituting glutamic or aspartic acid for Ser^{218} or Ser^{222}, the basal activity of MAPKK increased to four or eight times that of unphosphorylated wild-type enzyme, respectively (Fig. 1B). MAPKK incorporating both substitutions showed basal activity that was 85 times greater, thus demonstrating a synergistic effect (Fig. 1B).

A second gain-of-function mutation was identified by truncation of residues outside the kinase catalytic core. The NH_2-terminal region of MAPKK is predominantly hydrophilic and is rich in residues with a high propensity for α-helical folding (*13*). Deleting a predicted α helix encompassing residues 32 to 51 (Fig. 1A) resulted in a mutant, MAPKK(ΔN3), with basal activity 45 times greater than that of the wild-type enzyme (Fig. 1B). In contrast, the basal activities of two mutants with deletions spanning residues 1 to 32 (ΔN1) and 1 to 52 (ΔN2) were one-tenth that of the wild-type enzyme (*14*). Thus, residues 32 to 51 appear to stabilize the inactive state of MAPKK. This predicted α helix aligns with an α-helical motif, the A helix, that is found in several protein kinases, including cyclic adenosine 3′,5′-monophosphate (cAMP)–dependent protein kinase, casein kinase II, Src, Yes, Abl, Lck, the insulin receptor, and the platelet-derived growth factor receptor (Fig. 1A) (*15*). Our results implicate this motif in regulation of protein kinase activity.

Combining the ΔN3 deletion with the

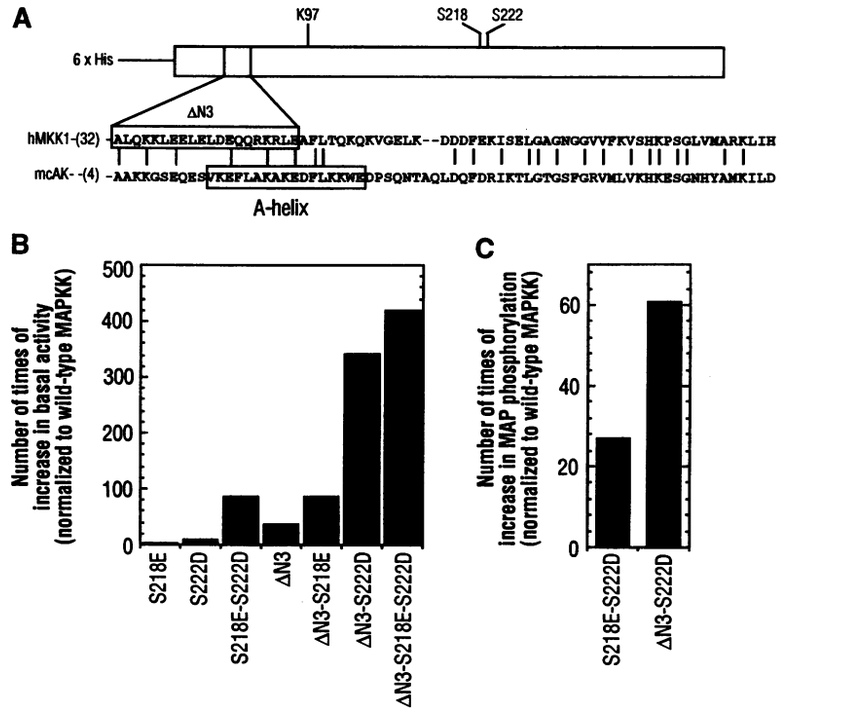

Fig. 1. Characterization of constitutively active MAPKK mutants. (**A**) Representation of the MAPKK fusion protein showing mutated residues. Residues 32 to 51 encompassing the ΔN3 deletion are aligned with the A-helix motif of mouse cAMP-dependent protein kinase (*15*, *19*). (**B**) Basal activities of bacterially expressed MAPKK proteins (*29*) were measured as the initial rates of phosphorylation of catalytically inactive rat ERK2(K52R) (*19*, *30*). MAPKK (20 ng) and ERK2(K52R) (800 ng) were incubated at 30°C in buffer A [10 mM Hepes (pH 7.4), 10 mM $MgCl_2$, 1 mM dithiothreitol, 0.1 mM adenosine triphosphate (ATP), and [γ-^{32}P]ATP (3000 cpm/pmol)] in a final volume of 20 μl. Reactions were terminated at various times by addition of Laemmli sample buffer. Proteins were separated by SDS–polyacrylamide gel electrophoresis (PAGE), and ^{32}P incorporation into ERK2(K52R) was quantified with a PhosphorImager. The basal activity of wild-type MAPKK was 0.4 nmol min^{-1} mg^{-1}. Each rate measurement represents the slope through three time points. Experiments were performed twice with similar results. (**C**) Activation of ERK2 by MAPKK mutants was normalized to the activation by wild-type MAPKK. Wild-type rat ERK2 (*30*) was preincubated with MAPKK for 20 min in buffer A, after which 10 μg of the ERK2 substrate, myelin basic protein, was added to the mixture. Reactions were terminated after an additional 10 min and ^{32}P incorporation into myelin basic protein was quantified as in (B).

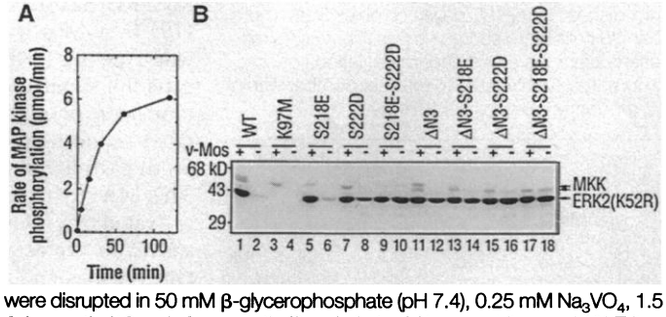

Fig. 2. Activation of wild-type and mutant MAPKK by v-Mos. MKK indicates full-length and truncated MAPKK. (**A**) Time course of MAPKK activation by v-Mos. Swiss 3T3 cells transformed with v-*mos* (cell line Tx-7) (*31*) were grown to confluence and treated with phorbol 12-myristate 13-acetate (0.1 μM) for 10 min at 37°C. Cells were disrupted in 50 mM β-glycerophosphate (pH 7.4), 0.25 mM Na_3VO_4, 1.5 mM EGTA, aprotinin (10 μg/ml), leupeptin (10 μg/ml), pepstatin (2 μg/ml), 1 mM benzamidine, and 1% Triton X-100 and clarified by centrifugation. The v-Mos protein was immunoprecipitated with a polyclonal antibody to Mos (residues 6 to 24) (*32*) bound to protein A–Sepharose resin. Kinase reactions (50 μl) were done by incubating the resin-bound v-Mos with MAPKK (0.3 μg) in buffer A at 30°C. At various times, the resin was sedimented by centrifugation and 35 μl of the supernatant (containing activated MAPKK) was added to 5 μl of ERK2(K52R) (0.5 mg/ml) and incubated for 5 min before termination and separation by SDS-PAGE. (**B**) Activation of wild-type and mutant MAPKK by v-Mos. Kinase reactions were carried out as in (A), except that MAPKK was incubated for 15 min in the presence (+) or absence (−) of v-Mos immunoprecipitates, after which supernatants containing MAPKK were removed and incubated with ERK2(K52R) for 15 min.

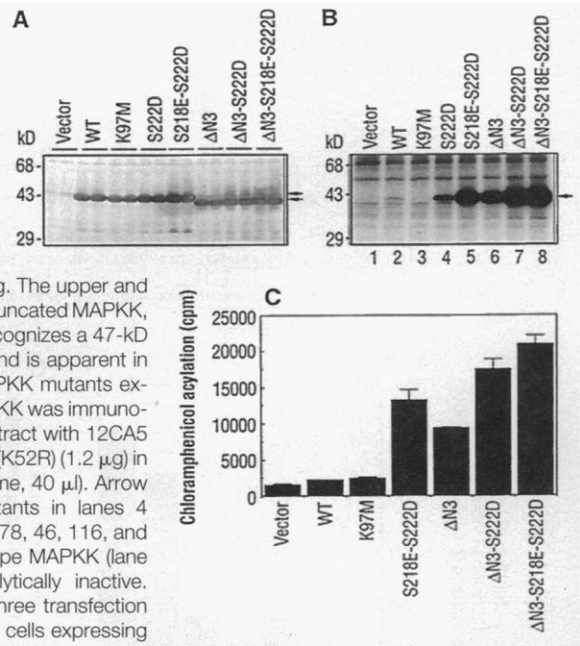

Fig. 3. Functional activity of MAPKK expressed in 293 cells. (**A**) Comparison of MAPKK expression. The 293 cells were transfected with constructs encoding HA-tagged MAPKK (*33*). Cells were lysed 44 hours after transfection, and expressed MAPKK in 25 μg of soluble extract was examined in duplicate by protein immunoblotting with monoclonal antibody 12CA5 (BabCo), which recognizes the HA tag. The upper and lower arrows indicate full-length and truncated MAPKK, respectively. Antibody 12CA5 also recognizes a 47-kD protein that is unrelated to MAPKK and is apparent in the vector control. (**B**) Activity of MAPKK mutants expressed in 293 cells. HA-tagged MAPKK was immunoprecipitated from 50 μg of soluble extract with 12CA5 and was used to phosphorylate ERK2(K52R) (1.2 μg) in buffer A for 12 min at 30°C (final volume, 40 μl). Arrow indicates ERK2(K52R). MAPKK mutants in lanes 4 through 8, respectively, exhibited 12, 78, 46, 116, and 176 times the basal activity of wild-type MAPKK (lane 2). MAPKK(K97M) (lane 3) is catalytically inactive. Equivalent results were obtained in three transfection experiments. (**C**) Activation of AP-1 in cells expressing MAPKK. Cells were transfected with MAPKK constructs and an AP-1–regulated CAT reporter construct (*32*). CAT activity was measured in cell extracts as counts per minute of [^{14}C]-butyryl coenzyme A (Dupont Biotechnology Systems) transferred to chloramphenicol in 30 min. Extracts containing 1 μg of protein were used in each assay.

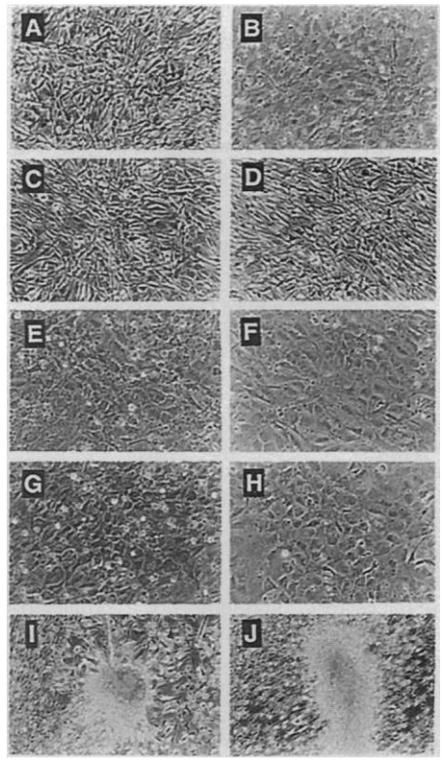

Fig. 4. Morphological transformation of NIH 3T3 cells. NIH/3T3 cells were stably transfected with (**A**) v-*mos*, (**B**) control selection vector, (**C**) HA-tagged MAPKK(ΔN3-S222D), (**D**) untagged MAPKK(ΔN3-S222D), (**E**) HA-tagged wild-type MAPKK, (**F**) untagged wild-type MAPKK, (**G**) HA-tagged catalytically inactive MAPKK(K97M), and (**H**) untagged MAPKK(K97M) (*20, 22*). Cells were seeded in 60-mm plates at a density of 2 × 10^5 cells per plate and grown for 12 days in 10% fetal bovine serum-DMEM. Foci were apparent in cells expressing (**I**) v-*mos* and (**J**) untagged MAPKK(ΔN3-S222D) and HA-tagged MAPKK(ΔN3-S222D) cells.

phosphorylation site substitutions enhanced basal MAPKK activity up to 410 times that of the wild-type enzyme (Fig. 1B). These MAPKK mutants stimulated wild-type MAPKs ability to phosphorylate myelin basic protein (Fig. 1C), which indicates that they phosphorylated the physiological regulatory sites on MAPK (*16*). Mass spectrometric analysis confirmed that MAPK (ERK2) was phosphorylated on Thr^{183} and Tyr^{185} (*17*).

Table 1. Focus formation and growth in soft agar of NIH 3T3 cells transfected with MAPKK. NIH 3T3 cells were stably transfected with each pMM9-MAPKK construct (*20*) or with v-*mos* (*22*) together with pSV2*neo* (Clontech) as described (*21*) and grown in the presence of geneticin (G418) (0.4 mg/ml) for 4 weeks. For focus formation assays, 2.0 × 10^5 cells were plated in triplicate onto 60-mm dishes, and after 16 days the number of foci on each dish were counted. For assays of anchorage-independent growth, 7.8 × 10^4 cells were plated in soft agar onto two 60 mm-dishes. After 16 days, colonies with more than 20 cells were scored as positive. Values represent averages and standard deviations of colony formation normalized to total cell number within 12 randomly selected fields of view.

Transfection	Focus formation (foci per dish)	Percent of cells forming colonies (out of total cells)
v-*mos*	352 ± 55	2.3 ± 1.2
pSV2*neo* control	0	0
Wild-type MAPKK + tag	0	0
Wild-type MAPKK − tag	0	0
MAPKK(K97M) + tag	0	0
MAPKK(K97M) − tag	0	0
MAPKK(ΔN3-S222D) + tag	11 ± 4	3.3 ± 1.8
MAPKK(ΔN3-S222D) − tag	138 ± 30	7.9 ± 3.1

We characterized the susceptibility of the constitutively active mutants to further activation by an upstream kinase, v-Mos, which, like Raf-1 and MEK kinase, may activate MAPKK by direct phosphorylation (*4, 5, 18*). The v-Mos phosphorylated and activated wild-type MAPKK (Fig. 2, A and B) and phosphorylated but did not activate the catalytically inactive MAPKK(K97M) (*19*) (Fig. 2B). Activation of the mutants MAPKK(S218E) (*19*) or MAPKK(S222D) (*19*) by v-Mos was comparable to that of wild-type MAPKK (Fig. 2B), which suggests full stimulation of each MAPKK mutant upon phosphorylation of the nonmutated serine residues; v-Mos had no effect on the activity of MAPKK(S218E-S222D). The MAPKK(ΔN3) deletion mutant was activated by v-Mos to a level matching that seen with the active, phosphorylated wild-type enzyme, and the activities of the compound mutants MAPKK(ΔN3-S218E), MAPKK(ΔN3-S222D), and MAPKK(ΔN3-S218E-S222D) were little affected by v-Mos.

In order to monitor their effects in intact cells, the MAPKK mutants were expressed in human kidney 293 cells under control of the cytomegalovirus (CMV) promoter. The amounts of exogenously expressed MAPKK protein were comparable, as judged from protein immunoblots of cell extracts (Fig. 3A). The basal activities of the constitutively active mutants were increased compared with that of the wild-type enzyme (Fig. 3B), correlating with the corresponding basal activities of bacterially expressed proteins (Fig. 1B). Because the transcription factor complex AP-1 is regulated by pathways that include MAPK (*9, 11*), we examined AP-1 activation by the MAPKK mutants using a reporter construct that directs transcription of chloramphenicol acetyltransferase (CAT). The amount of CAT expression (Fig. 3C) correlated with the activity of each mutant measured in vitro (Fig. 3B), demonstrating that the constitutively active MAPKK mutants were able to activate downstream signaling targets in intact cells.

Expression of constitutively active MAPKK led to morphological transformation of mammalian cells. NIH 3T3 cells were stably transfected with vectors encoding wild-type MAPKK, catalytically inac-

Table 2. Growth in nude mice of NIH/3T3 cells stably transfected with MAPKK. NIH 3T3 cells were transfected with pMM9-MAPKK (*20*) or with control vectors as in Table 1. Transfected cells selected for G418 resistance (1×10^6) were injected subcutaneously into the backs of weanling athymic nude mice as described (*21*). Tumor formation was monitored for up to 6 weeks. Mice in which tumors exceeded 20 mm in mean diameter were killed.

Transfection	Experiment no.	Tumor diameter (mm)			Number of mice with tumors compared with number of injected mice
		11 days	17 days	24 days	
v-*mos*	1	8.2 ± 2.5	24.0 ± 7.2	ND*	3/3
	2	0	9.3 ± 7.7	23.5 ± 2.1†	3/3
pSV2*neo* control	1	0	0	0	0/3‡
	2	0	0	0	0/3‡
Wild-type MAPKK + tag	1	0	0	0	0/3‡
	2	0	0	0	0/3‡
Wild-type MAPKK − tag	1	0	0	0	1/3§
	2	0	0	0	1/3‖
MAPKK(K97M) + tag	1	0	0	0	0/3‡
	2	0	0	0	0/3‡
MAPKK(K97M) − tag	1	0	0	0	0/3‡
	2	0	0	0	0/3‡
MAPKK(ΔN3-S222D) + tag	1	0	12.2 ± 1.5	24.5 ± 2.8	2/2
	2	0	6.8 ± 1.8	20.8 ± 2.5	3/3
	3	0	5.8 ± 3.2	19.3 ± 1.2	3/3
	4	0	5.7 ± 2.3	18.7 ± 6.3	3/3
MAPKK(ΔN3-S222D) − tag	1	0	7.0 ± 0.7	14.7 ± 6.6	3/3
	2	0	3.8 ± 1.4	16.0 ± 5.3	3/3
	3	0	6.0 ± 0.1	17.5 ± 0.7	2/2

*Not determined. Animals were killed before this time point. †Because one mouse was killed before this time point, data reflects $n = 2$. ‡After 42 days, none of the mice had formed tumors. §After 38 days, one mouse had formed an 8.5-mm tumor and two mice had no tumors. ‖After 38 days, one mouse had formed a 6-mm tumor and two mice had no tumors.

tive MAPKK(K97M), or constitutively active MAPKK(ΔN3-S222D), under control of the Moloney sarcoma virus long terminal repeat (MSV-LTR) (*20*, *21*). Two constructs were tested with each form of MAPKK; one encoded MAPKK fused to an NH_2-terminal hemagglutinin (HA) tag and the other was left untagged (*20*). Cells transfected with v-*mos* (*22*) or with the selection vector pSV2*neo* were used as positive and negative controls, respectively. After 3 weeks under selection, NIH 3T3 cells overexpressing v-*mos* (Fig. 4A) and cells transfected with MAPKK(ΔN3-S222D) (Fig. 4, C and D) showed many hallmarks of transformation, including cell rounding, high saturation density, loss of contact inhibition, and an unorganized growth pattern. In contrast, cells transfected with wild-type (Fig. 4, E and F) or catalytically inactive MAPKK (Fig. 4, G and H) showed a flattened morphology and a cobblestonelike growth pattern resembling that of untransformed control cells (Fig. 4B). Foci appeared in cells overexpressing v-*mos* (Fig. 4I and Table 1) or MAPKK(ΔN3-S222D) (Fig. 4J and Table 1) but not in control cells transfected with selection vector or with wild-type or catalytically inactive MAPKK (Table 1). Foci numbers were reduced in cells expressing HA-tagged MAPKK(ΔN3-S222D), as compared with the untagged mutant (Table 1). The activity of MAPKK(ΔN3-S222D), immunoprecipitated from cell extracts, was 55 times greater than that of wild-type MAPKK (*23*), which demonstrates that the morphological transformation correlated with enhanced kinase activity.

NIH 3T3 cells stably transfected with wild-type or mutant MAPKK were compared in two other assays for cell transformation. After cells were plated in soft agar, colonies were present in cells transfected with tagged or untagged MAPKK(ΔN3-S222D) and with v-*mos* but were absent in cells transfected with selection vector, wild-type MAPKK, or catalytically inactive MAPKK (Table 1). The tumorigenicity of transfected cells was also tested by direct injection into athymic nude mice (*21*). Solid tumors were observed within 2 weeks in mice injected with cells expressing MAPKK(ΔN3-S222D) (Table 2). In mice injected with cells expressing wild-type MAPKK or MAPKK(K97M), tumor growth was absent except for small tumors induced by wild-type MAPKK after 6 weeks (Table 2). The appearance of tumors within 2 weeks of injection demonstrates that the MAPKK(ΔN3-S222D) mutant is strongly oncogenic.

Signal transduction pathways regulated by oncogenes such as *ras*, *src*, *raf*, and *mos* proceed through the common activation of MAPKK and MAPK. However, these pathways may also branch into parallel kinase cascades. For example, the protein kinase JNK1 (or SAPK), like MAPK, activates AP-1 in response to overexpression of Ras (*24*). JNK1 is also regulated by phosphorylation but appears to be activated by a protein kinase that is distinct from MAPKK. Our findings indicate that although separate pathways diverge from Ras, constitutive activation of only one of these pathways is sufficient to transform cells.

Activation of the MAP kinase cascade is associated with signaling events that occur during the prereplicative growth (G_1) stage of the cell cycle, such as transcriptional regulation of immediate early gene expression (*6*, *8*, *9*), and could explain how oncogenes mediate the loss of growth control. In addition, MAPK is implicated in control of many G_2 to M transition events; for example, in the control of the interphase-metaphase transition of microtubule arrays (*25*), of cell rounding, and of chromosome condensation (*26*). These events also occur during interphase in transformed cells (*27*), which suggests that constitutively active MAPKK and MAPK may mediate the observed nuclear and cytoskeletal reorganization events.

Note added in proof: After acceptance of our manuscript, similar findings were reported by Cowley *et al.* (*28*).

REFERENCES AND NOTES

1. T. W. Sturgill, L. B. Ray, E. Erikson, J. L. Maller, *Nature* **334**, 715 (1988); J. S. Gregory, T. G. Boulton, B. C. Sang, M. H. Cobb, *J. Biol. Chem.* **264**, 18397 (1989); N. G. Ahn and E. G. Krebs, *ibid.* **265**, 11487 (1990); N. G. Ahn *et al.*, *ibid.* **266**, 4220 (1991); S. Matsuda *et al.*, *EMBO J.* **11**, 973 (1992).
2. N. Gomez and P. Cohen, *Nature* **353**, 170 (1991).
3. S. M. Thomas, M. DeMarco, G. D'Arcangelo, S. Halegoua, J. S. Brugge, *Cell* **68**, 1031 (1992); K. W. Wood, C. Sarnecki, T. M. Roberts, J. Blenis, *ibid.*, p. 1041; A. M. M. de Vreis-Smits, B. M. T. Burgering, S. J. Leevers, C. J. Marshall, J. L. Bos, *Nature* **357**, 602 (1992); D. J. Robbins *et al.*, *Proc. Natl. Acad. Sci. U.S.A.* **89**, 6924 (1992); C. Gallego, S. K. Gupta, L. E. Heasley, N. X. Qian, G. L. Johnson, *ibid.*, p. 7355.
4. J. M. Kyriakis *et al.*, *Nature* **358**, 417 (1992); P. Dent *et al.*, *Science* **257**, 1404 (1992); L. R. Howe *et al.*, *Cell* **71**, 335 (1992).
5. J. Posada, N. Yew, N. G. Ahn, G. F. Vande Woude, J. A. Cooper, *Mol. Cell. Biol.* **13**, 2546 (1993); E. K. Shibuya and J. V. Ruderman, *Mol. Biol. Cell* **4**, 781 (1993); A. Nebreda and T. Hunt, *EMBO J.* **12**, 1979 (1993).
6. R. J. Davis, *J. Biol. Chem.* **268**, 14553 (1993).
7. R.-H. Chen, C. Sarnecki, J. Blenis, *Mol. Cell. Biol.* **12**, 915 (1992); A. Seth, F. A. Gonzalez, S. Gupta, D. L. Raden, R. J. Davis, *J. Biol. Chem.* **267**, 24796 (1992); P. Lenormand *et al.*, *J. Cell Biol.* **122**, 1079 (1993).
8. B. J. Pulverer, J. M. Kyriakis, J. Avruch, E. Nikolakaki, J. R. Woodgett, *Nature* **353**, 670 (1991); E. Alvarez *et al.*, *J. Biol. Chem.* **266**, 15277 (1991).
9. H. Gille, A. D. Sharrocks, P. E. Shaw, *Nature* **358**, 414 (1992); R. Marias, J. Wynne, R. Treisman, *Cell* **73**, 381 (1993); T. Nakajima *et al.*, *Proc. Natl. Acad. Sci. U.S.A.* **90**, 2207 (1993).
10. G. Pages *et al.*, *Proc. Natl. Acad. Sci. U.S.A.* **90**, 8319 (1993); E. Sontag *et al.*, *Cell* **75**, 887 (1993); J. Troppmair *et al.*, *J. Biol. Chem.* **269**, 7030 (1994).
11. J. A. Frost, T. D. Geppert, M. H. Cobb, J. R. Feramisco, *Proc. Natl. Acad. Sci. U.S.A.* **91**, 3844 (1994).
12. C. F. Zheng and K. L. Guan, *EMBO J.* **13**, 1123 (1994); D. R. Alessi *et al.*, *ibid.*, p. 1610; K. A. Resing, S. J. Mansour, A. S. Hermann, N. G. Ahn, unpublished data.

13. K. T. O'Neil and W. F. DeGrado, *Science* **250**, 646 (1990).
14. Although the basal activities of the MAPKK(ΔN1) and MAPKK(ΔN2) mutants were less than that of wild-type MAPKK, the activities of these mutants after stimulation in vitro with v-Mos were similar to that of wild-type enzyme, which indicates that residues 1 to 51 are not required for MAPKK activity.
15. M. Veron, E. Radzio-Andzelm, I. Tsigelny, L. F. Ten Eyck, S. S. Taylor, *Proc. Natl. Acad. Sci. U.S.A.* **90**, 10618 (1993).
16. D. M. Payne *et al.*, *EMBO J.* **10**, 885 (1991).
17. K. A. Resing, A. S. Hermann, N. G. Ahn, unpublished data.
18. C. A. Lange-Carter, C. M. Pleiman, A. M. Gardner, K. J. Blumer, G. L. Johnson, *Science* **260**, 315 (1993).
19. Single-letter abbreviations for the amino acid residues are as follows: A, Ala; C, Cys; D, Asp; E, Glu; F, Phe; G, Gly; H, His; I, Ile; K, Lys; L, Leu; M, Met; N, Asn; P, Pro; Q, Gln; R, Arg; S, Ser; T, Thr; V, Val; W, Trp; and Y, Tyr.
20. MAPKK was subcloned into a derivative of pMB1, in which expression was driven by the MSV-LTR [D. G. Blair, W. L. McClements, M. K. Oskarsson, P. J. Fischinger, G. F. Vande Woude, *Proc. Natl. Acad. Sci. U.S.A.* **77**, 3504 (1980)]. The plasmid pMB1 was modified to introduce convenient restriction sites, yielding pMM9. To subclone untagged wild-type or mutant MAPKK into pMM9, the 1.5-kb Bam HI to Hind III fragment from pKH-1 was ligated with pMM9 that had been digested with Bam HI and Hind III. To subclone HA-tagged MAPKK into pMM9, the 1.6-kb Xba I to Hind III fragment from pMCL-MAPKK (*33*) was ligated with pMM9 that had been digested with Spe I and Hind III.
21. S. Rong *et al.*, *Mol. Cell. Biol.* **12**, 5152 (1992).
22. D. G. Blair *et al.*, *Cell* **46**, 785 (1986).
23. An equivalent amount of exogenously expressed MAPKK was observed in cell lines transfected with the HA-tagged constructs, as determined by protein immunoblotting with antibody 12CA5.
24. B. Derijard *et al.*, *Cell* **76**, 1025 (1994); J. M. Kyriakis *et al.*, *Nature* **369**, 156 (1994).
25. E. Nishida and Y. Gotoh, *Int. Rev. Cytol.* **138**, 211 (1992).
26. M. H. Verlhac, J. Z. Kubiak, H. J. Clarke, B. Maro, *Development* **120**, 1017 (1994).
27. N. Yew, M. Strobel, G. F. Vande Woude, *Curr. Opin. Genet. Dev.* **3**, 19 (1993).
28. S. Cowley, H. Paterson, P. Kemp, C. T. Marshall, *Cell* **77**, 841 (1994).
29. The bacterial expression construct pKH-1 encodes wild-type human MAPKK1 as a fusion protein with an NH_2-terminal hexahistidine tag (S. J. Mansour *et al.*, *J. Biochem.*, in press). Point mutations were introduced to generate the amino acid substitutions K97M, S218E, S222D, and S218E-S222D (*19*). To generate MAPKK(ΔN3), pKH-1 was digested with Stu I, and two fragments of 0.4 kb and 3.9 kb were recovered and ligated in the proper orientation, which resulted in the deletion of a 60–base pair (bp) fragment from the coding sequence. The ΔN3 deletion was combined with the various point mutations by replacement of a 0.9-kb Eco RI fragment in the ΔN3 construct with corresponding fragments from constructs containing the point mutations. Wild-type and mutant MAPKKs were purified by Ni^{2+}–nitrilotriacetic acid and DEAE chromatography as described (S. J. Mansour *et al.*, *J. Biochem.*, in press).
30. D. J. Robbins *et al.*, *J. Biol. Chem.* **268**, 5097 (1993).
31. K. Fukasawa *et al.*, *Cell Growth Differ.*, in press.
32. R. S. Paules, R. Buccione, R. C. Moschel, G. F. Vande Woude, J. J. Eppig, *Proc. Natl. Acad. Sci. U.S.A.* **86**, 5395 (1989).
33. Expression of genes in pCEP4-Lerner, modified from pCEP4 (Invitrogen), is driven by the CMV promoter and appends a nine–amino acid influenza HA tag at the NH_2-terminus of the expressed protein [I. Wilson *et al.*, *Cell* **37**, 767 (1984)]. The pCEP4-Lerner was modified to pMCL by introduction of convenient restriction sites, and a 1.5-kb Bam HI to Hind III fragment from pKH-1 (encoding wild-type MAPKK without the hexahistidine tag) was recovered and subcloned into pMCL digested with Bam HI and Hind III. The same approach was used to generate constructs encoding mutant HA-tagged MAPKK. We transfected the 293 cell line by electroporation with 15 μg of pMCL-MAPKK plasmid DNA. The efficiency of transfection was >80%. For CAT assays, cells were transfected with the pMCL-MAPKK plasmid (15 μg) and with the reporter plasmid pTE3ΔS-N (7.5 μg), which contains the CAT gene under control of 10 tandem repeats of the AP-1 site from SV40. Fresh medium was added to cells 24 hours after transfection. Twenty-four hours later, cell extracts were recovered and assays were done according to guidelines in the CAT Enzyme Assay System kit (Promega).
34. We thank L. Somparyac for assistance with soft agar assays; M. Kissinger and M. Oskarsson for assistance with cell culture; K. Resing for mass spectrometric analysis; M. Cobb, S.-C. Xu, and T. Geppert for ERK2 and the pCEP4-Lerner plasmid; M. Karin and A. Aronhein for the $pTE_3\Delta S$-N construct; M. Winey for 12CA5 antibodies; and A. Pardi, L. Sompayrac, and S. Berger for critical review of the manuscript. Supported by NIH grant GM48521 and the Searle Scholars Program (N.G.A.) and by the National Cancer Institute under contract N01-CO-74101 (G.F.V.W.).

24 May 1994; accepted 8 July 1994

Calcineurin Inhibition of Dynamin I GTPase Activity Coupled to Nerve Terminal Depolarization

Jun-Ping Liu,* Alistair T. R. Sim, Phillip J. Robinson

Dynamin I is a nerve terminal phosphoprotein with intrinsic guanosine triphosphatase (GTPase) activity that is required for endocytosis. Upon depolarization and synaptic vesicle recycling, dynamin I undergoes a rapid dephosphorylation. Dynamin I was found to be a specific high-affinity substrate for calcineurin in vitro. At low concentrations, calcineurin dephosphorylated dynamin I that had been phosphorylated by protein kinase C. The dephosphorylation inhibited dynamin I GTPase activity in vitro and after depolarization of nerve terminals. The effect in nerve terminals was prevented by the calcineurin inhibitor cyclosporin A. This suggests that in nerve terminals, calcineurin serves as a Ca^{2+}-sensitive switch for depolarization-evoked synaptic vesicle recycling.

Dynamin I (previously called dephosphin or p96) was discovered as a phosphoprotein in nerve terminals (*1*, *2*) and as a microtubule-binding protein with GTPase activity (*3*). Dynamin I is a family of four neural isoforms, dynamin II is a family of four isoforms expressed in most other tissues (*4*, *5*), and dynamin III is an apparently testis-specific form (previously called dynamin-2) (*6*, *7*). The GTPase activity of dynamin I is stimulated in vitro by microtubules (*8*, *9*), phospholipids (*10*), SH3 domain–containing proteins (*11*), and protein kinase C–mediated phosphorylation (*12*). Dynamin I is a good in vitro substrate of protein kinase C (Michaelis constant, K_m, of 0.35 μM) (*7*), and in resting nerve terminals, it is phosphorylated by this protein kinase (*13*). However, when synaptic vesicle recycling is stimulated by depolarization, dynamin I is dephosphorylated (*2*, *12*, *14*). Because mutations of the GTP-binding domain of dynamin I expressed in mammalian cells, or of the related dynamin family in the *Drosophila* mutant *shibire*, are defective in endocytosis (*15*–*18*), dynamin I and its phosphorylation control mechanisms are thus placed in the context of nerve terminal endocytosis (*12*). Endocytosis is a generalized intracellular pathway for the recycling of vesicle membrane from the plasma membrane, in which recycling vesicles are transiently surrounded by a protein coat of clathrin and adaptins, then invag-

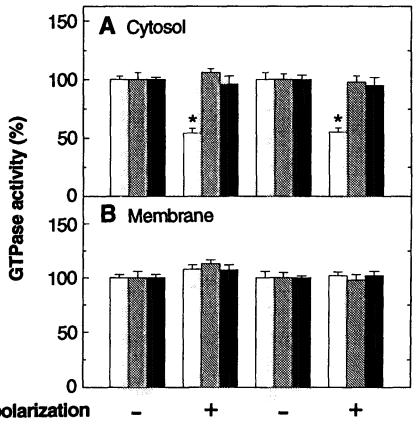

Fig. 1. Regulation of dynamin I GTPase activity in nerve terminals. Dynamin I was immunoprecipitated from isolated nerve terminals with specific antibodies and was assayed for GTPase activity before and after depolarization for 5 s with 41 mM K^+ in the presence of extracellular 0.1 mM Ca^{2+} (blank bar), 1 mM EGTA (striped bar), or 1 μM cyclosporin A (filled bar). (**A**) Dynamin I GTPase activity from the cytosolic fraction. (**B**) Dynamin I GTPase activity from the peripheral membrane fraction. Results are means of two experiments performed in quadruplicate. The asterisks indicate $P < 0.01$. For methods, see (*22*).

J.-P. Liu and P. J. Robinson, Endocrine Unit, John Hunter Hospital, Locked Bag 1, Hunter Region Mail Centre, NSW 2310, Australia.
A. T. R. Sim, The Neuroscience Group, The University of Newcastle, NSW 2308, Australia.
*To whom correspondence should be addressed.